



# Simulation of a Subjected Rigid Body Motion to an External Force and Moment

Asmaa Amer<sup>1</sup> · T. S. Amer<sup>2</sup> · A. A. Galal<sup>3</sup>

Received: 31 October 2022 / Revised: 16 April 2023 / Accepted: 11 May 2023 / Published online: 27 June 2023  
© The Author(s) 2023

## Abstract

**Purpose** This work intends to investigate the rigid body's motion around a specific fixed point (analogous to Lagrange's scenario) in the presence of a gyrostatic moment (GM) besides the attraction of a Newtonian force field (NFF). This task is carried out by presuming that the body is quickly rotating about one of the major or minor principal axes of the inertia ellipsoid.

**Method** The controlling system of six nonlinear differential equations (DEs) along with three first integrals is boiled down to an appropriate system of two DEs in addition to only one integral. Therefore, the analytic solutions of this system are obtained utilizing the approach of Poincaré small parameter (APSP).

**Results** Euler's angles for the motion under investigation are derived to assess this motion at any instant of time. Additionally, phase plane graphs are displayed using computer codes to depict the stability behavior of the dynamical motion at any time.

**Conclusion** These achieved outcomes are thought of as a generalization of the ones that were found in some of previous works, in the absence of all applied forces and moments. This work presents a distinctive contribution in several crucial areas, particularly in engineering applications that have used the gyroscopic theory to determine the orientation and maintain the stability of various vehicles, such as spaceships, airplanes, submarines, and racing cars.

**Keywords** Nonlinear dynamics · Rigid bodies · Perturbation approaches · Euler's angles · Newtonian force field · Gyrostatic moment

## Abbreviations

GM Gyrostatic moment  
NFF Newtonian force field  
DEs Differential equations  
AA Averaging approach  
AMS Approach of multiple scales

APSP Approach of Poincaré small parameter  
EMF Electromagnetic field

## Introduction

Researchers' interest has recently been drawn to study the problem of a rigid body (RB) in space. The reason is due to the diversity of its engineering, mechanical, and physics applications in daily life. Additionally, a great deal of scientific research has been done to examine the solutions to this problem. This problem demands complicated mathematical techniques because it is controlled by a nonlinear system of DEs besides three first integrals [1, 2]. The key challenge for researchers today is obtaining the full solution to this issue due to the difficulty of obtaining a general added fourth integral. This integral has been achieved for several special cases such as the cases of Euler, Lagrange, Kowalevski, Joukovsky, Volterra,

✉ T. S. Amer  
tarek.saleh@science.tanta.edu.eg

Asmaa Amer  
asmaaamer85@science.menofia.edu.eg

A. A. Galal  
abdallah.galal@f-eng.tanta.edu.eg

<sup>1</sup> Department of Mathematics and Computer Science, Faculty of Science, Menoufia University, Shebin El-Kom, Egypt

<sup>2</sup> Mathematics Department, Faculty of Science, Tanta University, Tanta 31527, Egypt

<sup>3</sup> Department of Physics and Engineering Mathematics, Faculty of Engineering, Tanta University, Tanta 31734, Egypt

Goryachev–Chaplygin, Kowalevski–Yehia’s case, and others. In these scenarios, both the location of the body’s center of mass and the magnitudes of the main moments of inertia are restricted. For more integrable scenarios, check out [2].

Since it is difficult or almost impossible, so far, to obtain the fourth integral in its full generality, attention has been directed toward the approximate solutions to this issue using the perturbation techniques [3–6] such as the approaches of Krylov–Bogoliubov–Mitropolski, multiple scales (AMS), averaging (AA), APSP, and others. These methods allow many researchers to obtain approximate solutions with great accuracy for the RB motion under the influence of different fields and moments.

The Krylov–Bogoliubov–Mitropolski is utilized in [7–10] to gain the approximate solutions of the rotatory motion of RB under the impact of a uniform gravitational field [7]. The obtained outcomes were generalized in [8] and [9] when the body is influenced by a GM and a Newtonian field of force, respectively. In [10], the authors constricted the body’s motion such that the body’s inertia ellipsoid is close to its inertia rotation. It should be noticed that the established solutions in [7] feature singular points when the body’s frequency has integer data or their inverses, while the corresponding ones in [8–10] do not have any singularities. The reason is due to that the authors of [7, 8] used Amer’s frequency which is dependent on the GM.

The AMS is used in a wide range of research related to the planar motion of a RB pendulum, e.g., [11–15] when its suspension is fixed [11], moves in a route of Lissajous curve [12], and moves on an elliptic route [13]. The motion’s regulating systems were obtained using Lagrange’s equations and solved according to the AMS procedure. The gained outcomes are graphed to show how different parameters affect the studied motion. Some of the resonance scenarios are grouped and examined in view of the obtained solvability criteria. The stability and instability criteria of Routh–Hurwitz [14] are used to examine the arisen fixed point. The numerical solutions of a RB pendulum are investigated in [15] near the equilibrium’s location. The motion of a triple RB pendulum with a fixed pivot point was studied in [16, 17] numerically and experimentally. The bifurcation and stability analysis, as well as numerical computing of a dynamical model with limiters rigid motion, are studied in [16]. In [17], it is demonstrated that the numerical and experimental results agree well for the motion of the same model.

The AA has been utilized frequently over the previous four decades to obtain solutions for the spinning motion of a symmetric RB, see [18–23]. This motion was investigated when the body is exposed to three different criteria: a uniform field of gravity, a NFF, and the existence of the

GM, as studied respectively, in [18–21], and [22, 23]. The authors have taken into their consideration the impact of the perturbing moments on the body’s motion. The fundamental equation of the body’s angular momentum is used to create the guiding equations of motion (EOM), in which a small parameter is inserted according to some applied hypothesis. The proper solutions of the AA systems of the corresponding ones of the EOM are obtained. In [22], it is considered that the inertia’s ellipsoid and rotations of the body are close to each other, in addition to the action of the electromagnetic field (EMF) on the body. The extension of this work is examined in [23], where the EOM are numerically examined by converting them to a system of two second-order DEs. The AA regulating system in [39] is solved numerically when the conditions of Lagrange’s gyroscope as well as some initial conditions of the angle of nutation are considered. The attained outcomes in [24] have been generalized in [25] and [26], when the applied perturbing moments slightly change over time and the body is exposed to external forces and moments, respectively. For additional details on how AA might be applied to address the RB’s problems, see [27].

The APSP, on the other hand, has been widely used in several studies e.g., [28–40] to obtain approximate solutions of a RB, whether the movement is considered under the influence of a gravitational field or a NFF, or in the presence of an EMF, or in the existence of the GM, or under the influence of a group of these forces and moments, or even under the influence of all of them. In [28, 29], the RB movement is examined in a field of uniform gravity, while the influence of the NFF on this motion is investigated in [30]. It must be noted that the obtained solutions comprised separate singular points when the system’s frequency had integer values or multiple inverses. These singularities have been treated forever in [31] when the motion is impacted only by the third component of the GM in addition to the NFF. In [32] and [33], the conditions of Euler–Poincaré and Kovalevskaya, respectively, were applied to the RB motion taking into account the influence of the entire GM. The achieved solutions are completely free of singularities at all for any value of the system’s frequency. Recently, this methodology is applied in [34] to investigate the movement of the RB in accordance with Bobylev–Steklov requirements, in which the body was being affected by the GM, EMF, and NFF. In [35], the authors proposed that the body’s center of mass is somewhat offset from its axis of dynamical symmetry when it is acted by the EMF and the GM. The gained results are considered a generic form of those which were obtained in [36] and [37]. For more information about how the strategy of this approach can be applied to address various SB’s problems, see [38] and [39].

The vibrations of the linear time-varying systems using some perturbation techniques have been studied in [40]. Based on analytical approximations of the relevant ordinary linear time-varying DEs, three conventional perturbation methods, namely the AA, harmonic balancing method, and AMS with linear scales have been employed. The accuracy of these techniques has been demonstrated by the study of vibrations with constant and increasing deployment velocities. Also, the dynamic properties of a deployable or retractable damped cantilever beam are examined experimentally and theoretically in [41]. Both the period decrement approach and the enveloped fitting method are used to calculate the time-varying damping as a function of the beam length.

The analytic approximate solutions for the governing equations for a restricted gyrostatic system are presented in [42] and [43] utilizing the large parameter technique. Some applications for the RB motion in a space have been examined in [44] when the body is supposed to be restricted under the influence gravity force, NFF, and GM. The stability is investigated for a free rotation of one-rotor gyrostat with the existence of internal moment in [45]. In an analogy way to Euler’s case, the lowest time of reducing rotation for a free dynamically asymmetric RB is examined in [46]. This body is affected by a one component of the GM and a viscous friction torque. The rotational law of optimal control for the sluggish body is defined, and the corresponding time and phase routes are assessed. The generalization of this problem is achieved in [47] when the body is acted by a full GM due to the action of three rotors, a small slowing viscous friction torque, and a minor control torque with close but unequal coefficients. An ideal decelerating law for the body’s rotation has been developed to control the body’s motion.

In this study, the movement of a RB around a fixed point that is near Lagrange’s gyroscope, under the impact of the NFF and the GM is investigated. The regulating EOM are derived in light of the principal angular momentum equation of the RB motion. This system is reduced via the APSP to one of two acceptable quasi-linear DEs from second order in terms of two variables only, and only one integral. The latter system is solved analytically, and therefore the other variables are achieved. The obtained outcomes are graphed according to various values of the body’s parameters to reveal the impact of these parameters on the motion’s behavior. Angles of Euler are derived to determine the orientation of the body at any instant. Furthermore, the plots of the phase plane are drawn to discuss the dynamical motion’s stability. This study’s significance stems from its wide-ranging applicability in life as well as in engineering applications where the gyroscopic theory has been used to establish the orientation and maintain the

stability of various vehicles such as submarines, spaceships, racing cars, and airplanes.

### Problem’s Depiction

This section presents a RB with mass  $M$  rotating in space around a specified fixed point  $O$  in the body, wherein it is regarded as an original of two Cartesian systems. The first one  $O\xi\eta\zeta$  is assumed to be fixed in space while the second frame  $Oxyz$  is fixed in the body’s structure and rotates with it and whose axes are running parallel to the inertia main axes. It should be mentioned that a quick rotation of the body around its  $z$ -axis has been considered to generate an angle  $\theta_0 \approx \pi/2$  with  $\zeta$ -axis. The body’s movement is controlled by an NFF that emerges from the center  $O_1$  at a significant distance  $R$  from  $O$ , in addition to the impact of the GM  $\underline{\ell} \equiv (\ell_x, 0, \ell_z)$  about the main inertia’s axes, see Fig. 1.

Let  $I \equiv (A^0(1 + \varepsilon\delta_1), A^0(1 + \varepsilon\delta_2), C)$  be the inertia moments tensor, where  $\delta_j (j = 1, 2)$  are dimensionless values of order unity,  $A^0$  stands for the unique value of inertia moments,  $C \neq A^0$  is the value of the inertia moment about  $z$ -axis, and  $\varepsilon$  is a tiny parameter. Moreover,  $r_G = (x_0, y_0, z_0)$  is the coordinates of the body’s center of mass,  $\underline{\Delta} = (\gamma, \gamma', \gamma'')$  denotes the cosine directions of the unit vector along  $\zeta$ -axis,  $\underline{\omega} \equiv (p, q, r)$  is the RB’s angular velocity along the principal axes  $(Ox, Oy, Oz)$ , and  $g$  is the gravitational acceleration. Therefore, the regulating system of the EOM can be constructed according to the principal equation of the body’s angular momentum  $\underline{h}_O$  and the first time derivative of the unit vector  $\underline{\Delta}$ , as shown below

$$\frac{d\underline{h}_O}{dt} + \underline{\omega} \wedge (\underline{h}_O + \underline{\ell}) = \underline{G}_O, \quad \frac{d\underline{\Delta}}{dt} = \underline{\Delta} \wedge \underline{\omega}. \tag{1}$$

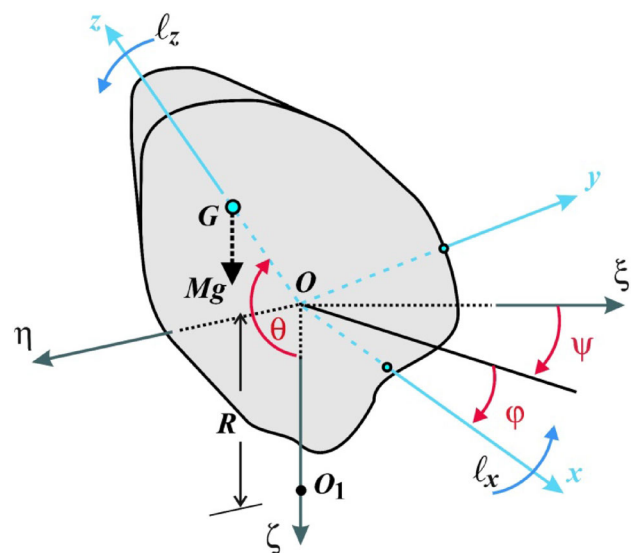


Fig. 1 Displays the problem’s dynamic design

where  $\underline{G}_O$  is an external force given by  $\underline{G}_O = Mg(r_{\underline{G}} \wedge \underline{\Delta}) + N(I\underline{\Delta} \wedge \underline{\Delta})$  and  $N = 3\lambda/R^3$ ,  $\lambda$  is the coefficient of the attracting center  $O_1$ .

The corresponding form to system of Eq. (1) is shown below

$$\begin{aligned} &A^0(1 + \varepsilon \delta_1) \frac{dp}{dt} + [C - A^0(1 + \varepsilon \delta_2)]qr + q\ell_z \\ &= Mg(y_0\gamma'' - z_0\gamma') + N[C - A^0(1 + \varepsilon \delta_2)]\gamma'\gamma'', \\ &A^0(1 + \varepsilon \delta_2) \frac{dq}{dt} + [A^0(1 + \varepsilon \delta_1) - C]rp + r\ell_x - p\ell_z \\ &= Mg(z_0\gamma - x_0\gamma'') + N[A^0(1 + \varepsilon \delta_1) - C]\gamma\gamma'', \\ &C \frac{dr}{dt} + A^0\varepsilon(\delta_2 - \delta_1)pq - q\ell_x \\ &= Mg(x_0\gamma' - y_0\gamma) + NA^0\varepsilon(\delta_2 - \delta_1)\gamma\gamma', \\ &\frac{d\gamma}{dt} = r\gamma' - q\gamma'', \frac{d\gamma'}{dt} = p\gamma'' - r\gamma, \frac{d\gamma''}{dt} = q\gamma - p\gamma', \end{aligned} \tag{2}$$

Based on the system of Eq. (2), the available first integrals have the forms

$$\begin{aligned} &A^0(1 + \varepsilon \delta_1)p^2 + A^0(1 + \varepsilon \delta_2)q^2 \\ &+ Cr^2 - 2Mg(x_0\gamma + y_0\gamma' + z_0\gamma'') \\ &+ N[A^0(1 + \varepsilon \delta_1)\gamma^2 + A^0(1 + \varepsilon \delta_2)\gamma'^2 + C\gamma''^2] \\ &= A^0(1 + \varepsilon \delta_1)p_0^2 + A^0(1 + \varepsilon \delta_2)q_0^2 \\ &+ Cr_0^2 - 2Mg(x_0\gamma_0 + y_0\gamma'_0 + z_0\gamma''_0) + N[A^0(1 + \varepsilon \delta_1)\gamma_0^2 \\ &+ A^0(1 + \varepsilon \delta_2)\gamma_0'^2 + C\gamma_0''^2], \\ &[A^0(1 + \varepsilon \delta_1)p + \ell_x]\gamma + A^0(1 + \varepsilon \delta_2)q\gamma' \\ &+ (Cr + \ell_z)\gamma'' = [A^0(1 + \varepsilon \delta_1)p_0 + \ell_x]\gamma_0 \\ &+ A^0(1 + \varepsilon \delta_2)q_0\gamma'_0 + (Cr_0 + \ell_z)\gamma''_0 \\ &\gamma^2 + \gamma'^2 + \gamma''^2 = 1, \end{aligned} \tag{3}$$

where  $p_0, q_0, r_0, \gamma_0, \gamma'_0$ , and  $\gamma''_0$  stand, respectively, for  $p, q, r, \gamma, \gamma',$  and  $\gamma''$  values at initial time.

To proceed with the body’s dynamical motion, the following presumptions are considered

$$\begin{aligned} &c\sqrt{\gamma''_0}p_1 = p, c\sqrt{\gamma''_0}q_1 = q, r_0r_1 = r, \gamma''_0\gamma_1 = \gamma, \\ &\gamma''_0\gamma'_1 = \gamma', \gamma''_0\gamma''_1 = \gamma'', \\ &x_0 = Lx'_0, y_0 = Ly'_0, z_0 = Lz'_0, \\ &L = |r_{\underline{G}}| = \sqrt{x_0^2 + y_0^2 + z_0^2}, \tau = r_0t, \\ &k = N\gamma''_0/c^2, c^2 = MgL/C, \varepsilon = c\sqrt{\gamma''_0}/r_0, \\ &A_1 = \frac{C - A^0(1 + \varepsilon \delta_2)}{A^0(1 + \varepsilon \delta_1)}, \\ &B_1 = \frac{A^0(1 + \varepsilon \delta_1) - C}{A^0(1 + \varepsilon \delta_2)}, C_1 = \frac{A^0\varepsilon(\delta_2 - \delta_1)}{C}, \\ &a = \frac{A^0(1 + \varepsilon \delta_1)}{C}, b = \frac{A^0(1 + \varepsilon \delta_2)}{C}, \\ &A_0 = (Ar_0)^{-1} = [A^0(1 + \varepsilon \delta_1)r_0]^{-1}, \\ &B_0 = (Br_0)^{-1} = [A^0(1 + \varepsilon \delta_2)r_0]^{-1}, C_0 = (Cr_0)^{-1}. \end{aligned} \tag{4}$$

where  $r_0$  has been assumed to be high and  $(x'_0, y'_0, z'_0)$  are dimensionless values.

The substitution of the presumptions (4) into the EOM (2) and integrals (3) yields

$$\begin{aligned} \dot{p}_1 + A_1q_1r_1 + A_0q_1\ell_z &= \varepsilon[a^{-1}(y'_0\gamma''_1 - z'_0\gamma'_1) + kA_1\gamma'_1\gamma''_1], \\ \dot{q}_1 + B_1r_1p_1 - B_0(p_1\ell_z - \varepsilon^{-1}r_1\ell_x) \\ &= \varepsilon[b^{-1}(z'_0\gamma_1 - x'_0\gamma''_1) + kB_1\gamma_1\gamma''_1], \\ \dot{r}_1 + \varepsilon^2C_1p_1q_1 - \varepsilon C_0q_1\ell_x &= \varepsilon^2(x'_0\gamma'_1 - y'_0\gamma_1 + kC_1\gamma_1\gamma'_1), \\ \dot{\gamma}_1 = r_1\gamma'_1 - \varepsilon q_1\gamma''_1, \quad \dot{\gamma}'_1 &= \varepsilon p_1\gamma''_1 - r_1\gamma_1, \\ \dot{\gamma}''_1 = \varepsilon(q_1\gamma_1 - p_1\gamma'_1), \end{aligned} \tag{5}$$

and

$$r_1^2 = 1 + \varepsilon^2S_1, r_1\gamma''_1 = 1 + \varepsilon S_2, \gamma_1^2 + \gamma_1'^2 + \gamma_1''^2 = (\gamma_0'')^{-2}. \tag{6}$$

Here, the dots denote the differentiation regarding to  $\tau$  and

$$\begin{aligned} S_1 &= a(p_{10}^2 - p_1^2) + b(q_{10}^2 - q_1^2) \\ &- 2[x'_{10}(\gamma_{10} - \gamma_1) + y'_{10}(\gamma'_{10} - \gamma'_1) + z'_{10}(1 - \gamma''_{10})] \\ &+ k[a(\gamma_{10}^2 - \gamma_1^2) + b(\gamma'_{10}{}^2 - \gamma_1'^2) + (1 - \gamma''_{10}{}^2)], S_2 \\ &= a(p_{10}\gamma_{10} - p_1\gamma_1) + b(q_{10}\gamma'_{10} - q_1\gamma'_1) \\ &+ (cC\sqrt{\gamma''_{10}})^{-1}[\ell_x(\gamma_{10} - \gamma_1) + \ell_z(1 - \gamma''_{10})], \end{aligned} \tag{7}$$

One can display  $S_1$  and  $S_2$  in expressions of power series of  $\varepsilon$  as follows

$$S_i = S_{i1} + 2^{2-i}\varepsilon S_{i2} + \dots, (i = 1, 2). \tag{8}$$

where

$$\begin{aligned} S_{11} &= a(p_{20}^2 - p_2^2) + bX^2(p_{20}^2 - p_2^2) - 2x'_0(\gamma_{20} - \gamma_2) - 2y'_0(\dot{\gamma}_{20} - \dot{\gamma}_2) \\ &+ k[a(\gamma_{20}^2 - \gamma_2^2) + b(\dot{\gamma}_{20}^2 - \dot{\gamma}_2^2)], \\ S_{12} &= a[\lambda(p_{20} - p_2) + \lambda_1(p_{20}\gamma_{20} - p_2\gamma_2)] \\ &- bX^2[a^{-1}y'_0(\dot{p}_{20} - \dot{p}_2) \\ &- \lambda_2(\dot{p}_{20}\dot{\gamma}_{20} - \dot{p}_2\dot{\gamma}_2)] - x'_0\rho_1(p_{20} - p_2) \\ &- y'_0\rho_2(\dot{p}_{20} - \dot{p}_2) + (z'_0 - k)S_{21} \\ &+ k[a\rho_1(p_{20}\gamma_{20} - p_2\gamma_2) + b\rho_2(\dot{p}_{20}\dot{\gamma}_{20} - \dot{p}_2\dot{\gamma}_2)], \\ S_{21} &= 2(p_{20}\gamma_{20} - p_2\gamma_2) - bX[(\dot{p}_{20}\dot{\gamma}_{20} - \dot{p}_2\dot{\gamma}_2) + y_1(\gamma_{20} - \gamma_2)], \\ S_{22} &= a[\rho_1(p_{20}^2 - p_2^2) + \lambda(\gamma_{20} - \gamma_2) + \lambda_1(\gamma_{20}^2 - \gamma_2^2)] \\ &+ b[-X\rho_2(\dot{p}_{20}^2 - \dot{p}_2^2) \\ &+ Xa^{-1}y'_0(\dot{\gamma}_{20} - \dot{\gamma}_2) - X\lambda_2(\dot{\gamma}_{20}^2 - \dot{\gamma}_2^2) \\ &+ y_1\rho_1(p_{20} - p_2) - y_3S_{21}], \end{aligned} \tag{9}$$

where

$$\begin{aligned}
 X &= A_1^{-1}(1 - A^{-1}A_1^{-1}r_0^{-1}\ell_z), \\
 \lambda &= x'_0b^{-1}\Omega^{-2}(A_1 + A^{-1}r_0^{-1}\ell_z), \\
 \lambda_1 &= (1 - \Omega^2)^{-1}[z'_0(A_1b^{-1} - a^{-1}) + k(A_1 - \omega^2) \\
 &\quad + (b^{-1}z'_0 + kB_1)A^{-1}r_0^{-1}\ell_z], \\
 \lambda_2 &= \lambda_1 + a^{-1}z'_0 - kA_1, \\
 \rho_1 &= (1 - \Omega^2)^{-1}(1 + B_1 - B^{-1}r_0^{-1}\ell_z), \\
 \rho_2 &= \rho_1 - X, \quad \Omega^2 = \omega^2 + (A_1B^{-1} - A^{-1}B_1)r_0^{-1}\ell_z, \\
 \omega^2 &= -A_1B_1, \\
 y_1 &= (cC\sqrt{\gamma''_0})^{-1}\ell_x, \quad y_3 = (cC\sqrt{\gamma''_0})^{-1}\ell_z
 \end{aligned}
 \tag{10}$$

The  $z$  and  $x$  axes' positive branches have been chosen in a way that prevents them from forming an obtuse angle with the  $\zeta$ -axis direction, i.e.,

$$y_0 \geq 0, 0 < \gamma''_0 < 1. \tag{11}$$

### System's Reduction Processes

The specific objective of this section is to reduce the equations of system (5) and integrals (6) to another suitable quasi-linear system of two second-order DEs and only one integral. To achieve this goal,  $r_1$  and  $\gamma''_1$  must be rewritten in the following way while taking integrals (6) into account

$$\begin{aligned}
 r_1 &= 1 + \frac{1}{2} \varepsilon^2 S_{11} + \dots, \\
 \gamma''_1 &= 1 + \varepsilon S_{21} + \varepsilon^2(S_{22} - \frac{1}{2} S_{11}) + \dots,
 \end{aligned}
 \tag{12}$$

In this context, we differentiate the first and fourth Equations in (5) and then using (12) to yield

We can infer from a close examination of the two equations above that they have frequencies of  $\Omega$  and 1. Amer's frequency [31] is the name given to the frequency  $\Omega$ , and it has a real value. The terms  $r_0^{-2}, r_0^{-3}, \dots$  can be disregarded because it has been assumed that  $r_0$  would have a large value. Therefore, using the formulas in (5) and (12), we may rewrite  $q_1$  and  $\gamma'_1$  as follows

$$\begin{aligned}
 q_1 &= (A_1^{-1}r_1^{-1} - A_1^{-2}A^{-1}r_0^{-1}r_1^{-2}\ell_z + \dots) \\
 &\quad [ \varepsilon a^{-1}(y'_0\gamma''_1 - z'_0\gamma'_1 + kA_1\gamma'_1\gamma''_1) - \dot{p}_1 ], \\
 \gamma'_1 &= r_1^{-1}(\dot{\gamma}_1 + \varepsilon q_1 \gamma''_1).
 \end{aligned}
 \tag{15}$$

Introducing  $p_2$  and  $\gamma_2$  as two additional variables

$$p_2 = p_1 - \varepsilon(\lambda + \lambda_1 \gamma_2), \quad \gamma_2 = \gamma_1 - \varepsilon \rho_1 p_2, \tag{16}$$

then we can write  $q_1$  and  $\gamma'_1$  in terms of  $p_2, \gamma_2, \dot{p}_2$ , and  $\dot{\gamma}_2$  as follows

$$\begin{aligned}
 q_1 &= -X\dot{p}_2 + \varepsilon[X(a^{-1}y'_0 - \lambda_2\dot{\gamma}_2)] + \varepsilon^2\{X[(kA_1 - a^{-1}z'_0)\rho_1 + S_{11}]\dot{p}_2 \\
 &\quad - \frac{1}{2}A_1^{-1}S_{11}\dot{p}_2 + XS_{21}(kA_1\dot{\gamma}_2 + a^{-1}y'_0)\} + \dots, \\
 \gamma'_1 &= \dot{\gamma}_2 + \varepsilon\rho_2\dot{p}_2 + \varepsilon^2[X(a^{-1}y'_0 - \lambda_2\dot{\gamma}_2 - S_{21}\dot{p}_2) - \frac{1}{2}S_{11}\dot{\gamma}_2] + \dots,
 \end{aligned}
 \tag{17}$$

The substitution of (8), (9), (12), (16), and (17) into (13) and (14) produces the following quasi-linear autonomous system with two degrees of freedom and just one integral,

$$\begin{aligned}
 \ddot{p}_2 + \Omega^2 p_2 &= CA_1B^{-1}y_1 + \varepsilon F(p_2, \dot{p}_2, \gamma_2, \dot{\gamma}_2, \varepsilon), \\
 \ddot{\gamma}_2 + \gamma_2 &= B^{-1}r_0^{-1}\ell_x + \varepsilon \Phi(p_2, \dot{p}_2, \gamma_2, \dot{\gamma}_2, \varepsilon),
 \end{aligned}
 \tag{18}$$

and

$$\begin{aligned}
 \gamma_2^2 + \dot{\gamma}_2^2 + 2\varepsilon(\rho_1\gamma_2 p_2 + S_{21}) \\
 + \varepsilon^2\{\rho_1^2 p_2^2 + \rho_2^2 \dot{p}_2^2 + 2\dot{\gamma}_2[A_1^{-1}(a^{-1}y'_0 - \lambda_2\dot{\gamma}_2 - \dot{p}_2 S_{21}) \\
 - \frac{1}{2}S_{11}\dot{\gamma}_2] + S_{21}^2 + 2(S_{22} - \frac{1}{2}S_{11})\} = (\gamma''_0)^{-2} - 1.
 \end{aligned}
 \tag{19}$$

$$\begin{aligned}
 \ddot{p}_1 + \Omega^2 p_1 &= \varepsilon^{-1}(A_1B^{-1}r_0^{-1}\ell_x) + \varepsilon\{-C^{-1}A_1r_0^{-1}\ell_x q_1^2 + A_1B^{-1}r_0^{-1}\ell_x S_1 + z'_0(a^{-1} - A_1b^{-1})\gamma_1 \\
 &\quad + A_1b^{-1}x'_0 + k(\omega^2 - A_1)\gamma_1 + [b^{-1}(x'_0 - z'_0\gamma_1) - kB_1\gamma_1]A^{-1}r_0^{-1}\ell_z\} + \varepsilon^2\{-\omega^2 p_1 S_1 \\
 &\quad + A^{-1}b^{-1}x'_0 S_2 + A_1 C_1 p_1 q_1^2 - A_1 x'_0 \gamma'_1 q_1 + A_1 y'_0 q_1 \gamma_1 + a^{-1} y'_0 q_1 \gamma_1 - a^{-1} y'_0 p_1 \gamma'_1 \\
 &\quad - a^{-1} z'_0 p_1 + A_1 k[p_1(1 - \gamma_1^2) + q_1(1 - C_1)\gamma_1 \gamma'_1 - S_2(1 + B_1)\gamma_1] + \frac{1}{2}r_0^{-1}\ell_z p_1(A^{-1}B_1 \\
 &\quad - A_1B^{-1})[S_1 + 2z'_0(1 - \gamma_1) - k(1 - \gamma_1^2)] + A^{-1}r_0^{-1}\ell_z(b^{-1}x'_0 - kB_1\gamma_1)S_2\} + \dots,
 \end{aligned}
 \tag{13}$$

$$\begin{aligned}
 \ddot{\gamma}_1 + \gamma_1 &= B_0\ell_x + \varepsilon[B_0\ell_x S_2 + p_1(1 + B_1 - B_0\ell_z) + C_0\gamma'_1 q_1 \ell_x] + \varepsilon^2[(1 + B_1)p_1 S_2 \\
 &\quad - \gamma_1 S_1 - B_0 p_1 \ell_z S_2 + p_1 q_1 \gamma'_1(1 - C_1) + x'_0 \gamma_1^2 - y'_0 \gamma_1 \gamma'_1 - z'_0 b^{-1} \gamma_1 + b^{-1} x'_0 \\
 &\quad - q_1^2 \gamma_1 + k(C_1 \gamma_1^2 - B_1) \gamma_1] + \dots,
 \end{aligned}
 \tag{14}$$

Here

$$\begin{aligned}
 &F = F_1 + \varepsilon F_2 + \varepsilon^2 F_3 + \dots, \Phi = \Phi_1 + \varepsilon \Phi_2 + \varepsilon^2 \Phi_3 + \dots, \\
 &F_1 = -\lambda B^{-1} r_0^{-1} \ell_x - C^{-1} r_0^{-1} A_1^{-1} \ell_x \dot{p}_2^2 + A_1 B^{-1} r_0^{-1} \ell_x S_{11} + z'_0 (a^{-1} - A_1 b^{-1}) \gamma_2 + A_1 b^{-1} x'_0 \\
 &\quad + k(\omega^2 - A_1) \gamma_2 + (b^{-1} x'_0 - b^{-1} z'_0 \gamma_2 - k B_1 \gamma_2) A^{-1} r_0^{-1} \ell_z, \\
 &F_2 = f_2 - \rho_1 \lambda_1 (1 - \Omega^2) p_2, F_3 = f_3 - \lambda_1 \varphi_2 - \rho_1 \lambda \lambda_1 (1 - \Omega^2) - \rho_1 \lambda_1^2 \gamma_2 (1 - \Omega^2), \\
 &\Phi_1 = B^{-1} r_0^{-1} \ell_x S_{21} - C^{-1} r_0^{-1} \ell_x \dot{\gamma}_2 A_1^{-1} \dot{p}_2, \\
 &\Phi_2 = \rho_1 (1 - \Omega^2) (\lambda + \lambda_1 \gamma_2) + \phi_2, \Phi_3 = \phi_3 - \rho_1 f_2 - \rho_1^2 \lambda_1 (1 - \Omega^2) p_2, \\
 &f_2 = 2A_1 B^{-1} r_0^{-1} \ell_x S_{12} + (A_1 b^{-1} x'_0 S_{21} - \omega^2 S_{11} p_2) + A_1 C_1 p_2 A_1^{-2} [\dot{p}_2^2 - 2\dot{p}_2 (a^{-1} y'_0 - \lambda_2 \dot{\gamma}_2)] \\
 &\quad + x'_0 \dot{\gamma}_2 \dot{p}_2 - y'_0 A_1^{-1} (A_1 + a^{-1}) \dot{p}_2 \gamma_2 - a^{-1} y'_0 p_2 \dot{\gamma}_2 - a^{-1} z'_0 p_2 + A_1 k p_2 (1 - \dot{\gamma}_2^2 - 2\dot{\gamma}_2 \rho_1 \dot{p}_2) \\
 &\quad + k \gamma_2 \dot{\gamma}_2 \dot{p}_2 (C_1 - 1) - A_1 k \gamma_2 S_{21} (1 + B_1) + \frac{1}{2} r_0^{-1} \ell_z p_2 S_{11} (A^{-1} B_1 - A_1 B^{-1}) + \rho_1 \lambda_1 C A_1 B^{-1} y_1 \\
 &\quad - \lambda_1 (B^{-1} r_0^{-1} \ell_x S_{21} - C^{-1} r_0^{-1} \ell_x \dot{\gamma}_2 A_1^{-1} \dot{p}_2), \\
 &\varphi_2 = B^{-1} r_0^{-1} \ell_x S_{22} - C^{-1} r_0^{-1} \ell_x \rho_2 \dot{p}_2^2 A_1^{-1} + C^{-1} r_0^{-1} A_1^{-1} \ell_x \dot{\gamma}_2 (a^{-1} y'_0 - \lambda_2 \dot{\gamma}_2) - \gamma_2 S_{11} \\
 &\quad + (1 + B_1 - B^{-1} r_0^{-1} \ell_z) p_2 S_{21} - (1 - C_1) p_2 \dot{\gamma}_2 A_1^{-1} \dot{p}_2 + x'_0 \dot{\gamma}_2^2 - y'_0 \gamma_2 \dot{\gamma}_2 - z'_0 b^{-1} \gamma_2 \\
 &\quad + x'_0 b^{-1} - \gamma_2 X^2 \dot{p}_2^2 + k C_1 \gamma_2 \dot{\gamma}_2^2 - k B_1 \gamma_2, \\
 &f_3 = C^{-1} r_0^{-1} A_1^{-1} \ell_x (a^{-1} y'_0 - \lambda_2 \dot{\gamma}_2)^2 - (2\omega^2 p_2 S_{12} - A_1 b^{-1} x'_0 S_{22}) - \omega^2 S_{11} (\lambda + \lambda_1 \gamma_2) \\
 &\quad + A_1^{-1} C_1 (\lambda + \lambda_1 \gamma_2) [\dot{p}_2^2 - 2\dot{p}_2 (a^{-1} y'_0 - \lambda_2 \dot{\gamma}_2)] - x'_0 \dot{\gamma}_2 (a^{-1} y'_0 - \lambda_2 \dot{\gamma}_2) + x'_0 \rho_1 \dot{p}_2^2 \\
 &\quad - \rho_1 p_2 \dot{p}_2 y'_0 A_1^{-1} (A_1 + a^{-1}) - a^{-1} y'_0 p_2 (\rho_1 \dot{p}_2 + q_1) - a^{-1} y'_0 \dot{\gamma}_2 (\lambda + \lambda_1 \gamma_2) - a^{-1} z'_0 (\lambda \\
 &\quad + \lambda_1 \gamma_2) + A_1 k (\lambda + \lambda_1 \gamma_2) (1 - \dot{\gamma}_2^2 - 2\dot{\gamma}_2 \rho_2 \dot{p}_2) + A_1 k (1 - C_1) [\gamma_2 \dot{\gamma}_2 (A^{-1} a^{-1} y'_0 - \lambda_2 \dot{\gamma}_2) \\
 &\quad - A_1^{-1} \gamma_2 \rho_1 \dot{p}_2^2 - \rho_1 p_2 A_1^{-1} \dot{\gamma}_2 \dot{p}_2] - A_1 k S_{22} \gamma_2 (1 + B_1) - A_1 k S_{11} \rho_1 p_2 (1 + B_1) + \frac{1}{2} r_0^{-1} \ell_z \\
 &\quad \times (A^{-1} B_1 - A_1 B^{-1}) [p_2 (2S_{12} - 2z'_0 S_{21} + 2k S_{21}) + (\lambda + \lambda_1 \gamma_2) S_{11}] + \frac{1}{2} z'_0 (a^{-1} - A_1 b^{-1}) \\
 &\quad \times \gamma_2 S_{11} + \frac{1}{2} A^{-1} r_0^{-1} \ell_z (k B_1 \gamma_2 - b^{-1} x'_0) S_{11} + (2k A_1 - a^{-1} z'_0) S_{21} p_2 + A_1 B^{-1} r_0^{-1} \ell_x S_{11} \\
 &\quad + \rho_1 \lambda_1 z'_0 (a^{-1} - A_1 b^{-1}) \gamma_2 + \rho_1 \lambda_1 A_1 b^{-1} x'_0 + k \rho_1 \lambda_1 (\omega^2 - A_1) \gamma_2 + \rho_1 \lambda_1 (b^{-1} x'_0 - b^{-1} z'_0 \gamma_2 \\
 &\quad - k B_1 \gamma_2) A^{-1} r_0^{-1} \ell_z - \rho_1 \lambda_1 \omega^2 (\lambda + \lambda_1 \gamma_2), \\
 &\varphi_3 = -C^{-1} r_0^{-1} A_1^{-2} \ell_x \dot{p}_2 (a^{-1} y'_0 - \lambda_2 \dot{\gamma}_2 - \dot{p}_2 S_{21} - \frac{1}{2} S_{11} A_1 \dot{\gamma}_2) + C^{-1} r_0^{-1} \ell_x \dot{\gamma}_2 \{ [A_1^{-1} (k A_1 - a^{-1} z'_0) \rho_1 \\
 &\quad + A_1^{-1} S_{11}] \dot{p}_2 - \frac{1}{2} A_1^{-1} S_{11} \dot{p}_2 + A_1^{-1} (k A_1 \dot{\gamma}_2 + a^{-1} y'_0) S_{21} \} + C^{-1} r_0^{-1} A_1^{-1} \ell_x \rho_2 \dot{p}_2 (a^{-1} y'_0 - \lambda_2 \dot{\gamma}_2) \\
 &\quad - \rho_1 p_2 S_{11} - 2\gamma_2 S_{12} + (1 + B_1 + B^{-1} r_0^{-1} \ell_z) [p_2 S_{22} + (\lambda + \lambda_1 \gamma_2) S_{21}] + (1 - C_1) p_2 A_1^{-1} \\
 &\quad \times (a^{-1} y'_0 - \lambda_2 \dot{\gamma}_2) \dot{\gamma}_2 - (1 - C_1) p_2 A_1^{-1} \rho_2 \dot{p}_2^2 - (1 - C_1) \dot{p}_2 \dot{\gamma}_2 A_1^{-1} (\lambda + \lambda_1 \gamma_2) + 2x'_0 \dot{\gamma}_2 \rho_2 \dot{p}_2 \\
 &\quad - y'_0 \gamma_2 \rho_1 \dot{p}_2 - y'_0 \rho_1 p_2 \dot{\gamma}_2 - z'_0 b^{-1} \rho_1 p_2 + 2\gamma_2 A_1^{-2} \dot{p}_2 (a^{-1} y'_0 - \lambda_2 \dot{\gamma}_2) - \rho_1 p_2 A_1^{-2} \dot{p}_2^2 + 2k C_1 \\
 &\quad \times \gamma_2 \dot{\gamma}_2 \rho_2 \dot{p}_2 + k C_1 \rho_1 p_2 \dot{\gamma}_2^2 - k B_1 \rho_1 p_2 + 2b^{-1} x'_0 S_{21} - b^{-1} z'_0 \gamma_2 S_{21} - 2k B \gamma_2 S_{21} - \frac{1}{2} B^{-1} r_0^{-1} \\
 &\quad \times \ell_z p_2 [S_{11} + 2z'_0 (1 - \gamma_1'') - k (1 - \gamma_1''^2)].
 \end{aligned} \tag{20}$$

The generating form of system (18) has the form

$$\ddot{p}_2^{(0)} + \Omega^2 p_2^{(0)} = 0, \quad \ddot{\gamma}_2^{(0)} + \gamma_2^{(0)} = 0, \tag{22}$$

which allows solutions with period  $T_0 = 2\pi n$  fill out the form

$$p_2^{(0)} = M_1 \cos \Omega \tau + M_2 \sin \Omega \tau, \quad \gamma_2^{(0)} = M_3 \cos \tau, \tag{23}$$

where  $M_j$  ( $j = 1, 2, 3$ ) are determinable constants.

Based on the preceding, the desirable solutions of system (18) can be assumed in the following form with period  $T(\varepsilon) = T_0 + \alpha(\varepsilon)$

### Formalization of the Periodic Solution

Determining the periodic solutions of (18) while accounting for the positive sign of  $\Omega^2$  is the main objective of this section. According to the autonomy of this system, it is evident that the below requirements have no bearing on the generality of the solutions  $p, q, r, \gamma, \gamma'$ , and  $\gamma''$ .

$$p_2(0, 0) = C A_1 B^{-1} y_1, \quad \dot{p}_2(0, 0) = 0, \quad \dot{\gamma}_2(0, \varepsilon) = 0. \tag{21}$$



$$\begin{aligned}
 p_2(\tau, \varepsilon) &= (M_1 + \beta_1) \cos \Omega \tau + (M_2 + \beta_2) \sin \Omega \tau + \sum_{n=1}^{\infty} \varepsilon^n G_n(\tau), \\
 \gamma_2(\tau, \varepsilon) &= (M_3 + \beta_3) \cos \tau + \sum_{n=1}^{\infty} \varepsilon^n H_n(\tau), \\
 g_n(\tau) &= \frac{1}{\Omega} \int_0^{\tau} F_n^{(0)}(t_1) \sin \Omega(\tau - t_1) dt_1, \\
 h_n(\tau) &= \int_0^{\tau} \Phi_n^{(0)}(t_1) \sin(\tau - t_1) dt_1, \quad (n = 1, 2),
 \end{aligned}
 \tag{24}$$

where  $\beta_1, \Omega\beta_2$ , and  $\beta_3$  denote the initial value’s deviation of  $p_2, \dot{p}_2$ , and  $\gamma_2$  for the system (18) from their corresponding values of the system (22). These variations are functions of  $\varepsilon$ , in which they are vanishing at  $\varepsilon = 0$ . One may establish the required criteria for these solutions (22) at  $t = 0$  by the relations given below

$$\begin{aligned}
 p_2(0, \varepsilon) &= M_1 + \beta_1, & \dot{p}_2(0, \varepsilon) &= \Omega(M_2 + \beta_2), \\
 \gamma_2(0, \varepsilon) &= M_3 + \beta_3, & \dot{\gamma}_2(0, \varepsilon) &= 0.
 \end{aligned}
 \tag{25}$$

Using the next operator, the functions  $G_n(\tau)$  and  $H_n(\tau)$ , ( $n = 1, 2, 3, \dots$ ) can be identified as follows [48]

$$\begin{aligned}
 D &= d + \frac{\partial d}{\partial M_1} \beta_1 + \frac{\partial d}{\partial M_2} \beta_2 + \frac{\partial d}{\partial M_3} \beta_3 + \frac{1}{2} \frac{\partial^2 d}{\partial M_1^2} \beta_1^2 + \dots; \\
 \begin{pmatrix} D \\ d \end{pmatrix} &= \begin{pmatrix} G_n, H_n \\ g_n, h_n \end{pmatrix}.
 \end{aligned}
 \tag{26}$$

The function  $g_j(\tau)$  and  $h_j(\tau)$  adopt the following forms.

where

$$\begin{aligned}
 F_n^{(0)}(\tau) &= \frac{1}{(n-1)!} \left( \frac{d^{n-1} F}{d\varepsilon^{n-1}} \right)_{\varepsilon=0}, & \Phi_n^{(0)}(\tau) \\
 &= \frac{1}{(n-1)!} \left( \frac{d^{n-1} \Phi}{d\varepsilon^{n-1}} \right)_{\varepsilon=0}.
 \end{aligned}$$

It is worthy to mention that system (18), as seen in its right sides, starts with a small parameter of order zero. Consequently, we can determine the functions  $F_n^{(0)}$  and  $\Phi_n^{(0)}$  as follows

$$\begin{aligned}
 F_n^{(0)} &= F_n(p_2^{(0)}, \dot{p}_2^{(0)}, \gamma_2^{(0)}, \dot{\gamma}_2^{(0)}), & \Phi_n^{(0)} \\
 &= \Phi_n(p_2^{(0)}, \dot{p}_2^{(0)}, \gamma_2^{(0)}, \dot{\gamma}_2^{(0)}); \quad (n = 1, 2).
 \end{aligned}$$

In view of the above, solutions (23) can be rewritten as

$$\begin{aligned}
 p_2^{(0)} &= E \cos(\Omega\tau - \eta), & \gamma_2^{(0)} &= M_3 \cos \tau; \\
 E &= \sqrt{M_1^2 + M_2^2}, & \mu &= \tan^{-1} M_2/M_1.
 \end{aligned}
 \tag{28}$$

The substitution of (28) into (9) yields

$$\begin{aligned}
 S_{11}^{(0)} &= E^2 [a(\cos^2 \eta - \frac{1}{2}) + bX^2\Omega^2(\sin^2 \eta - \frac{1}{2}) + \frac{1}{2}(bX^2\Omega^2 - a) \cos 2(\Omega\tau - \eta)] \\
 &\quad - 2M_3[x'_0(1 - \cos \tau) + y'_0 \sin \tau] - \frac{1}{2}kM_3^2 C_1(1 - \cos 2\tau), \\
 S_{21}^{(0)} &= M_3 E [a \cos \eta + \frac{1}{2}(bX\Omega - a) \cos[(\Omega - 1)\tau - \eta] - \frac{1}{2}(bX\Omega + a) \\
 &\quad \times \cos[(\Omega + 1)\tau - \eta]] + M_3 y_1(1 - \cos \tau), \\
 S_{12}^{(0)} &= aE \{ \lambda [\cos \eta - \cos(\Omega\tau - \eta)] + \lambda_1 M_3 \cos \eta - \frac{1}{2} \lambda_1 M_3 \cos [(\Omega + 1)\tau - \eta] \\
 &\quad + \cos [(\Omega - 1)\tau - \eta] \} - bX^2 E \Omega \{ a^{-1} y'_0 [\sin \eta + \sin(\Omega\tau - \eta)] + \frac{\lambda^2}{2} M_3 \\
 &\quad \times [\cos((\Omega - 1)\tau - \eta) - \cos((\Omega + 1)\tau - \eta)] \} - x'_0 \rho_1 E [\cos \eta - \cos(\Omega\tau - \eta)] \\
 &\quad - y'_0 \rho_2 E \Omega [\sin \eta + \sin(\Omega\tau - \eta)] + (z'_0 - k) S_{21}^{(0)} + k \rho_1 E M_3 \{ \cos \eta \\
 &\quad - \frac{1}{2} [\cos((\Omega + 1)\tau - \eta) + \cos((\Omega - 1)\tau - \eta)] - \frac{1}{2} k b \rho_2 E M_3 \Omega \{ \cos [(\Omega - 1)\tau - \eta] - \cos [(\Omega + 1)\tau - \eta] \}, \\
 S_{22}^{(0)} &= a \rho_1 E^2 \{ \cos^2 \eta - \frac{1}{2} [1 + \cos 2(\Omega\tau - \eta)] \} + a \lambda M_3 (1 - \cos \tau) + \frac{1}{2} \lambda_1 M_3^2 \\
 &\quad \times (1 - \cos \tau) \} - bX \rho_2 E^2 \Omega^2 \{ \sin^2 \eta - \frac{1}{2} [1 - \cos 2(\Omega\tau - \eta)] \} + bX a^{-1} y'_0 M_3 \sin \tau \\
 &\quad + \frac{1}{2} bX \lambda_2 M_3^2 (1 - \cos 2\tau) + y_1 \rho_1 E [\cos \eta - \cos(\Omega\tau - \eta)] - y_3 S_{21}^{(0)}.
 \end{aligned}
 \tag{29}$$

Substituting (28) and (29) into (20), we get

$$\begin{aligned}
 F_1^{(0)} &= 0, \\
 \Phi_1^{(0)} &= -y_1 r_0^{-1} B^{-1} \ell_x M_3 \cos \tau + \dots, \\
 F_2^{(0)} &= L(\Omega) (M_1 \cos \Omega \tau + M_2 \sin \Omega \tau) + \dots, \\
 \Phi_2^{(0)} &= M_3 N(\Omega) \cos \tau + \dots,
 \end{aligned}
 \tag{30}$$

where

$$\begin{aligned}
 L(\Omega) &= A_1 k - [a^{-1} z_0' + \rho_1 \lambda_1 (1 - \Omega^2)] \\
 &\quad - 2a A_1 \lambda r_0^{-1} B^{-1} \ell_x + \left[ \frac{1}{2} r_0^{-1} \ell_z (A^{-1} B_1 \right. \\
 &\quad \left. - A_1 B^{-1}) - \omega^2 \right] [a M_1^2 + b X^2 \Omega^2 M_2^2 \\
 &\quad - \frac{1}{2} (a + b X^2 \Omega^2) - 2 M_3 x_0'] \\
 &\quad - \frac{1}{2} k M_3^2 C_1 - \frac{1}{2} (b X^2 \Omega^2 - a) (M_1^2 + M_2^2)] + \dots, \\
 N(\Omega) &= -(a M_1^2 + b X^2 \Omega^2 M_2^2) \\
 &\quad + (1 + b) (M_1^2 + M_2^2) X^2 \Omega^2 + 2 x_0' M_3 \\
 &\quad - [b^{-1} z_0' - \rho_1 \lambda_1 (1 - \Omega^2)] \\
 &\quad + k \left( \frac{1}{2} M_3^2 C_1 - B_1 \right) - a \lambda r_0^{-1} B^{-1} \ell_x + \dots.
 \end{aligned}
 \tag{31}$$

The functions  $g_n, \dot{g}_n, h_n$ , and  $\dot{h}_n$  ( $n = 1, 2$ ) can be obtained using the expressions (27), (30), and (31) as follows

$$\begin{aligned}
 g_1(T_0) &= 0, \quad g_2(T_0) = -\pi n \Omega^{-1} M_2 L(\Omega), \\
 \dot{g}_1(T_0) &= 0, \quad \dot{g}_2(T_0) = \pi n M_1 L(\Omega), \\
 h_1(T_0) &= 0, \quad h_2(T_0) = 0, \quad \dot{h}_1(T_0) = 0, \\
 \dot{h}_2(T_0) &= \pi n M_3 N(\Omega).
 \end{aligned}
 \tag{32}$$

The proposed solutions (24) and their related first derivatives must satisfy the following constraints for periodicity to acquire  $M_j, \beta_i$ , and the correction  $\alpha$  of the period.

$$\begin{aligned}
 \psi_1 &= p_2(T_0 + \alpha, \varepsilon) - p_2(0, \varepsilon) = 0, \\
 \psi_2 &= \dot{p}_2(T_0 + \alpha, \varepsilon) - \dot{p}_2(0, \varepsilon) = 0, \\
 \psi_3 &= \gamma_2(T_0 + \alpha, \varepsilon) - \gamma_2(0, \varepsilon) = 0, \\
 \psi_4 &= \dot{\gamma}_2(T_0 + \alpha, \varepsilon) - \dot{\gamma}_2(0, \varepsilon) = 0.
 \end{aligned}
 \tag{33}$$

Notably, the existence of the integral (19) is related to the above mentioned third condition  $\psi_3 = 0$ . Accordingly, one can use the criteria (25) and (33) to get

$$2 (M_3 + \beta_3) \psi_3 + \psi_3^2 + \varepsilon h_1(\psi_1, \psi_2, \psi_3, \psi_4, \varepsilon) = 0. \tag{34}$$

In this case,  $h_1$  stands for an entire function where  $h_1(0, 0, 0, \varepsilon) = 0$ . When  $M_3 \neq 0$ , we obtain  $\psi_3 =$

$k_1(\psi_1, \psi_2, \psi_3, \psi_4, \varepsilon)$ , where  $k_1$  is a function that fulfills the condition  $k_1(0, 0, 0, 0, \varepsilon) = 0$ . Then the condition  $\psi_3 = 0$  in (34) is compatible with the removal of the other conditions, i.e.,

$$\psi_1 = \psi_2 = \psi_4 = 0. \tag{35}$$

At  $\tau = 0$ , the substitution of (25) into (19) yields

$$\begin{aligned}
 M_3^2 + 2 M_3 \beta_3 + \beta_3^2 + 2 \varepsilon \rho_1 (M_1 + \beta_1) (M_3 + \beta_3) + \dots \\
 = (\gamma_0'')^{-2} - 1.
 \end{aligned}$$

If  $\gamma_0''$  is independent of  $\varepsilon$ , then  $M_3$  and  $\beta_3$  can be produced in the following forms

$$\begin{aligned}
 M_3 &= (1 - \gamma_0''^2)^{1/2} (\gamma_0'')^{-1}, \quad 0 < M_3 < \infty, \quad \beta_3 \\
 &= -\varepsilon \rho_1 (M_1 + \beta_1) + \dots.
 \end{aligned}
 \tag{36}$$

By disregarding terms of order  $\alpha^2$  and extending the conditions (33) regarding  $\alpha$  power series, we obtain

$$\begin{aligned}
 p_2(T_0, \varepsilon) + \alpha \dot{p}_2(T_0, \varepsilon) + \dots - p_2(0, \varepsilon) &= 0, \\
 \dot{p}_2(T_0, \varepsilon) + \alpha \ddot{p}_2(T_0, \varepsilon) + \dots - \dot{p}_2(0, \varepsilon) &= 0, \\
 \dot{\gamma}_2(T_0, \varepsilon) + \alpha \ddot{\gamma}_2(T_0, \varepsilon) + \dots - \dot{\gamma}_2(0, \varepsilon) &= 0.
 \end{aligned}$$

Utilizing the criteria (25) into the aforementioned relations, the independent conditions of periodicity (35) can be rewritten as follows

$$\begin{aligned}
 p_2(T_0, \varepsilon) + \alpha \Omega (M_2 + \beta_2) - (M_1 + \beta_1) &= 0, \\
 \dot{p}_2(T_0, \varepsilon) - \Omega (M_2 + \beta_2) + \alpha \Omega^2 (M_1 + \beta_1) + \alpha C B^{-1} A_1 y_1 &= 0, \\
 \dot{\gamma}_2(T_0, \varepsilon) - \alpha (M_3 + \beta_3) + \alpha r_0^{-1} B^{-1} \ell_x &= 0.
 \end{aligned}
 \tag{37}$$

The correction of period  $\alpha(\varepsilon)$  can be achieved after using (24) and (36) besides the last equation of (37), in the form

$$\begin{aligned}
 \alpha(\varepsilon) &= \varepsilon (M_3 + \beta_3 - r_0^{-1} B^{-1} \ell_x)^{-1} (\dot{F}_1(T_0) + \varepsilon \dot{F}_2(T_0) \\
 &\quad + \varepsilon^2 \dot{F}_3(T_0) + \dots).
 \end{aligned}
 \tag{38}$$

Utilizing (24), (32), and the first two equations of (37) and (38) to create the below system that determines  $\beta_1$  and  $\beta_2$

$$\begin{aligned}
 -\pi n \beta_2 \Omega^{-1} \{L_1(\Omega) - \Omega^2 N_1(\Omega) \\
 [1 + (r_0^{-1} B^{-1} \ell_x) (M_3 + \beta_3 - r_0^{-1} B^{-1} \ell_x)^{-1}]\} \\
 + \varepsilon (G_2(T_0) + \dots) &= 0, \\
 \pi n \beta_1 \{L_1(\Omega) + N_1(\Omega) (C A_1 B^{-1} y_1 - \Omega \beta_1) \\
 [1 + (r_0^{-1} B^{-1} \ell_x) (M_3 + \beta_3 - r_0^{-1} B^{-1} \ell_x)^{-1}]\} \\
 + \varepsilon [\dot{G}_2(T_0) + \dots] &= 0.
 \end{aligned}
 \tag{39}$$



**Table 1** Shows the relevant data which are used to display the temporary motion and phase plane plots in various graphs

$M$	$x'_0$	$y'_0$	$z'_0$	$\delta_1$	$\delta_2$	$R$	$\gamma''_0$	$A_0$	$C$	$r_0$	$\gamma_0$
300 kg	0.7 m	0.3 m	0.1 m	50	45	1000 m	0.001	15	11	5 rad. s <sup>-1</sup>	0.001

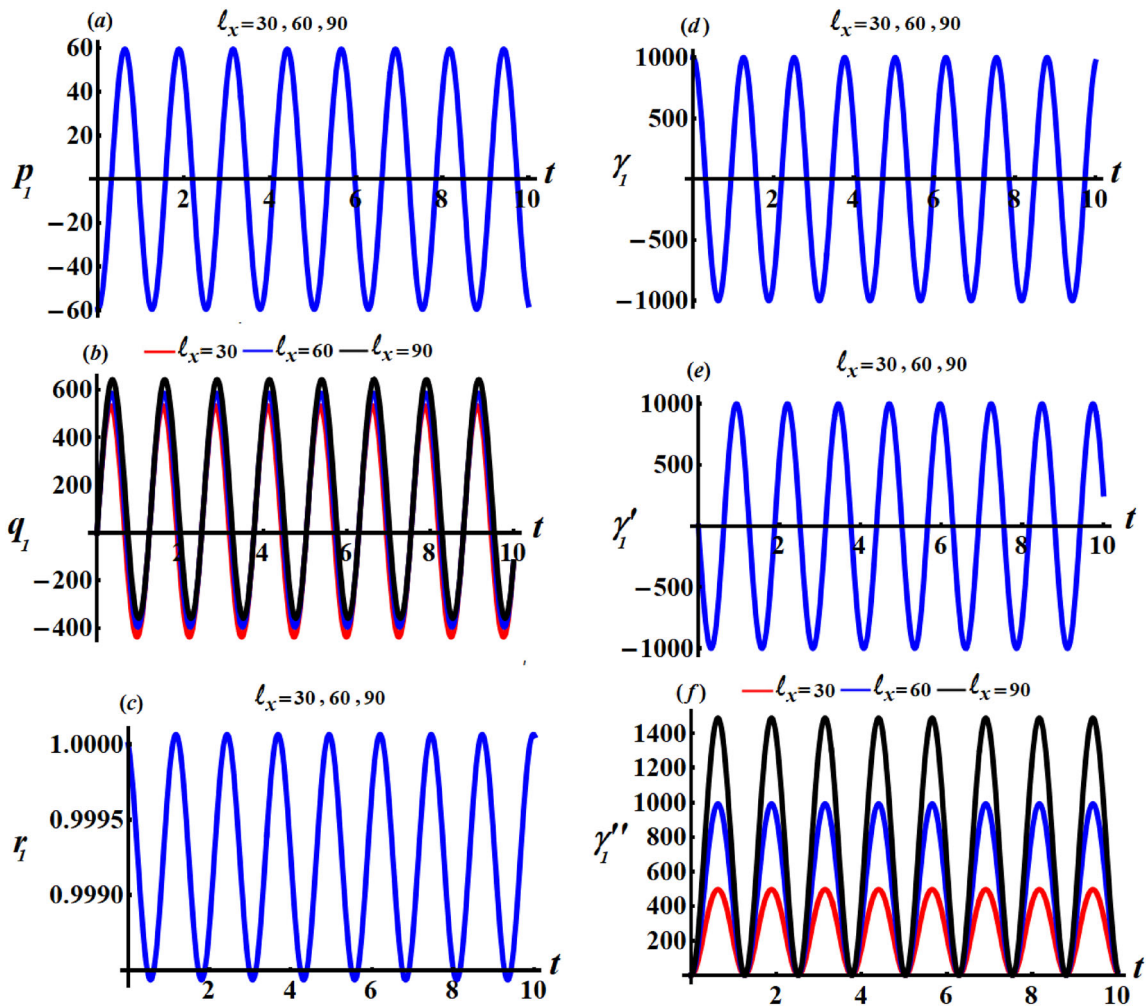


**Fig. 2** The time history of the obtained approximate solutions  $p_1, q_1, r_1, \gamma_1, \gamma'_1$ , and  $\gamma''_1$  over time  $t$  when  $l_z = 30 \text{ kg m}^2 \text{ s}^{-1}$  with different values of  $l_x (= 30, 60, 90) \text{ kg m}^2 \text{ s}^{-1}$

Replacing  $M_1, M_2, M_3$  by  $\beta_1, \beta_2, M_3 + \beta_3$ , respectively, the functions  $L_1(\Omega)$  and  $N_1(\Omega)$  can be obtained as follows

$$L_1(\Omega) - \Omega^2 N_1(\Omega) = (\beta_1^2 + \beta_2^2) W_1(\Omega) + z'_0 W_2(\Omega) + kW_3(\Omega) + W_4(\Omega), \tag{40}$$

where

$$\begin{aligned} W_1(\Omega) &= \frac{1}{2} (b\Omega^2 X^2 - a)(\Omega^2 + \frac{1}{2}y) - (1+b)\Omega^4 X^2, \\ W_2(\Omega) &= b^{-1}\Omega^2 - a^{-1}, \\ W_3(\Omega) &= A_1 + \frac{1}{4}C_1 y (M_3 + \beta_3)^2 + \Omega^2 \beta_1, \\ W_4(\Omega) &= B^{-1}r_0^{-1} a \lambda l_x (\Omega^2 - 2A_1) \\ &\quad - \rho_1 \lambda_1 (1 - \Omega^4) + \frac{1}{2}y [\frac{1}{2}(a + b\Omega^2 X^2) \\ &\quad + 2x'_0 (M_3 + \beta_3) + (a\beta_1^2 + b\Omega^2 X^2 \beta_2^2)] + \frac{1}{2}\Omega^2 (a + b\Omega^2 X^2) \end{aligned}$$

Based on (39), it is possible to get the formulations for  $\beta_n$  ( $n = 1, 2$ ) in terms of  $\epsilon$  whose first terms begin with

$O(\varepsilon^3)$ . Consequently, the periodic solutions up to the first approximate order have the following forms

interval. As a result, we may formulate Euler’s angles as follows [1]

$$\begin{aligned}
 p_1 &= \varepsilon\{\Omega^{-2}[x'_0 b^{-1}(A_1 + A^{-1}r_0^{-1}\ell_z)] + \lambda_1 M_3 \cos \tau\} + \dots, \\
 q_1 &= \varepsilon X(a^{-1}y'_0 + \lambda_2 M_3 \sin \tau) + \varepsilon^2 X(a^{-1}y'_0 - kA_1 M_3 \sin \tau)[M_3 y_1(1 - \cos \tau)] + \dots, \\
 r_1 &= 1 + \frac{1}{2} \varepsilon^2 \{-2M_3[x'_0(1 - \cos \tau) + y'_0 \sin \tau] - \frac{1}{2}kM_3^2 C_1(1 - \cos 2\tau)\} + \dots, \\
 \gamma_1 &= M_3 \cos \tau + \dots, \\
 \gamma'_1 &= -M_3 \sin \tau + \varepsilon^2 \{X(a^{-1}y'_0 + \lambda_2 M_3 \sin \tau) - \frac{1}{2}M_3 \sin \tau[2M_3[x'_0(1 - \cos \tau) + y'_0 \sin \tau] \\
 &\quad + \frac{1}{2}kM_3^2 C_1(1 - \cos 2\tau)]\} + \dots, \\
 \gamma''_1 &= 1 + \varepsilon[M_3 y_1(1 - \cos \tau)] + \varepsilon^2 \{a\lambda M_3(1 - \cos \tau) + \frac{1}{2}M_3^2(1 - \cos 2\tau)(a\lambda_1 + bX\lambda_2) \\
 &\quad + bXa^{-1}y'_0 M_3 \sin \tau - M_3 y_1 y_3(1 - \cos \tau) + M_3[x'_0(1 - \cos \tau) + y'_0 \sin \tau] \\
 &\quad + \frac{1}{4}kM_3^2 C_1(1 - \cos 2\tau)\} + \dots, \\
 \alpha(\varepsilon) &= \varepsilon \pi n [1 + (M_3 + \beta_3 - r_0^{-1}B^{-1}\ell_x)^{-1}(r_0^{-1}B^{-1}\ell_x)][2x'_0 M_3 - z'_0 b^{-1} + \rho_1 \lambda_1(1 - \Omega^2) \\
 &\quad + k(\frac{1}{2}M_3^2 C_1 - B_1) - r_0^{-1}B^{-1}a\lambda\ell_x] + \dots.
 \end{aligned}
 \tag{41}$$

A closer examination of the aforementioned solutions revealed that they exhibit periodic behaviors with various values of the gyrostat’s physical parameters. It is emphasized that for any rational value of the frequency  $\Omega$ , the gained solutions do not have any singular point. The reason is going back to the use of the frequency of Amer that depends on the third projection of the GM on the  $z$ -axis. As seen from the mathematical forms of these solutions, we expect that the waves of these solutions will behave the forms of periodic waves, due to that these results include trigonometric functions. Moreover, the solutions  $p_1$ ,  $q_1$ , and  $\gamma''_1$  will be varied with the GM values owing to that these solutions include the components  $\ell_x$  and  $\ell_z$  of the GM.

### Rigid Body Orientations

The goal of the current section is to demonstrate the RB’s orientation at any specific instant in view of the achieved solutions and angles of Euler. Such angles are specified by the angles of nutation, self-rotation, and precession, that are always represented as  $\theta$ ,  $\varphi$ , and  $\psi$ , respectively.

In light of the fact that system (18) is regarded as autonomous (18), the acquired solutions (41) will remain periodic if  $t$  is changed to  $(t + t_0)$ , where  $t_0$  denotes any

$$\begin{aligned}
 \cos \theta &= \gamma'', \quad \frac{d\psi}{dt} = \frac{p\gamma + q\gamma'}{1 - \gamma'^2}, \quad \tan \varphi_0 = \frac{\gamma_0}{\gamma'_0}, \\
 \frac{d\varphi}{dt} &= r - \frac{d\psi}{dt} \cos \theta.
 \end{aligned}
 \tag{42}$$

The required Euler’s angles for the investigated problem can be obtained by at once substituting (4) and (41) into (42)

$$\begin{aligned}
 \phi_0 &= (\pi/2) + r_0 h + \dots, \quad \theta_0 = \tan^{-1} M_3, \\
 \theta &= \theta_0 - \varepsilon [\theta_1(t+h) - \theta_1(h)] - \varepsilon^2 [\theta_2(t+h) - \theta_2(h)], \\
 \psi &= \psi_0 + c \cos \theta_0 \sqrt{\cos \theta_0} \{ [\psi_1(t+h) - \psi_1(h)] \\
 &\quad + \varepsilon [\psi_2(t+h) - \psi_2(h)] \\
 &\quad + \varepsilon^2 [\psi_3(t+h) - \psi_3(h)] \}, \\
 \phi &= \phi_0 + r_0 t - c \cot \theta_0 \sqrt{\cos \theta_0} \{ [\phi_1(t+h) - \phi_1(h)] \\
 &\quad + \varepsilon [\phi_2(t+h) - \phi_2(h)] \} \\
 &\quad - \varepsilon^2 \{ \tan \theta_0 [\phi_3(t+h) - \phi_3(h)] \\
 &\quad + c \cot \theta_0 \sqrt{\cos \theta_0} [\phi_4(t+h) - \phi_4(h)] \},
 \end{aligned}
 \tag{43}$$

where

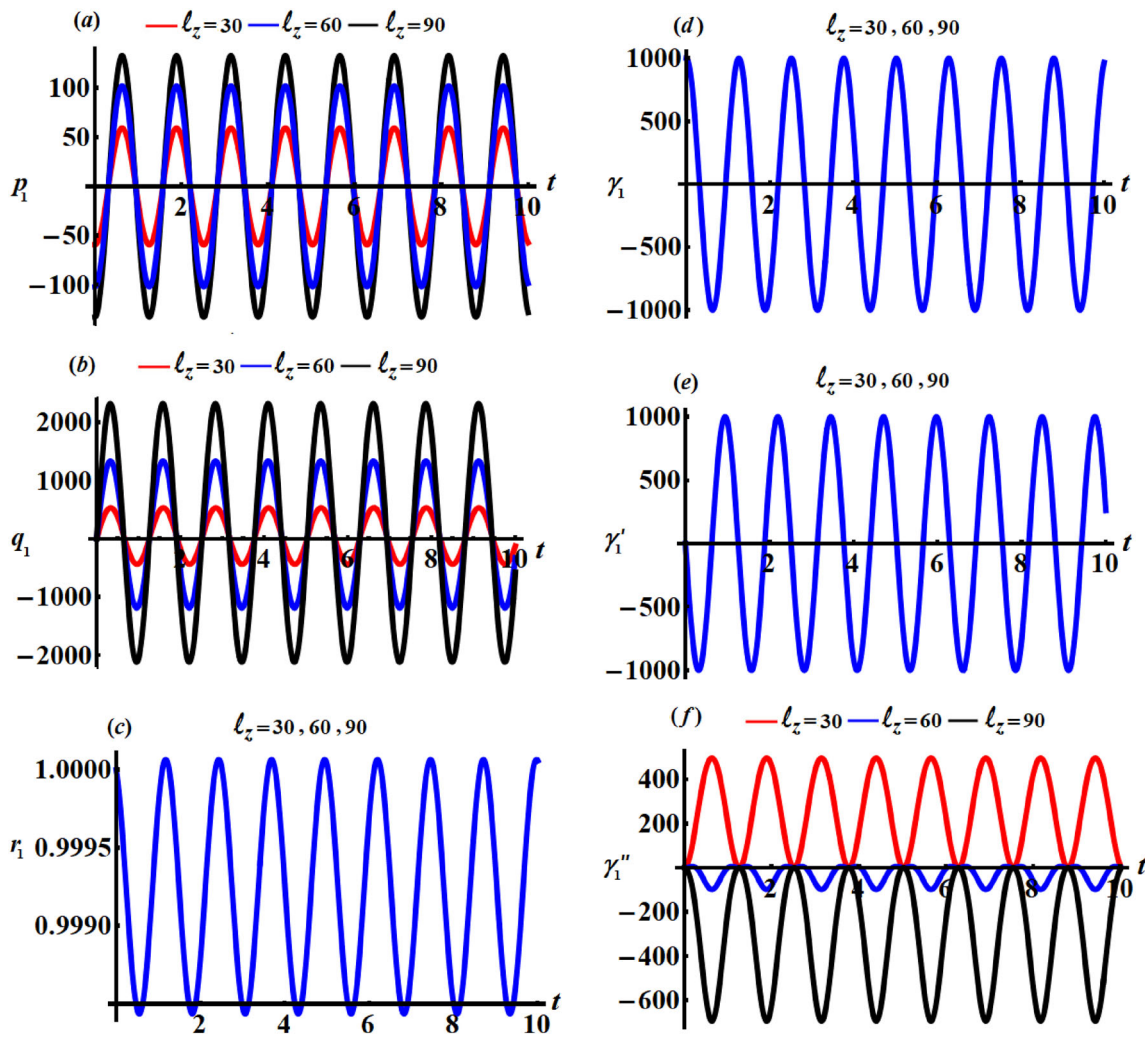


**Fig. 3** The fluctuation of  $p_1, q_1, r_1, \gamma_1, \gamma_1',$  and  $\gamma_1''$  versus  $t$  when  $l_x = 30 \text{ kg m}^2 \text{ s}^{-1}$  with the increase of  $l_z (= 30, 60, 90) \text{ kg m}^2 \text{ s}^{-1}$  values

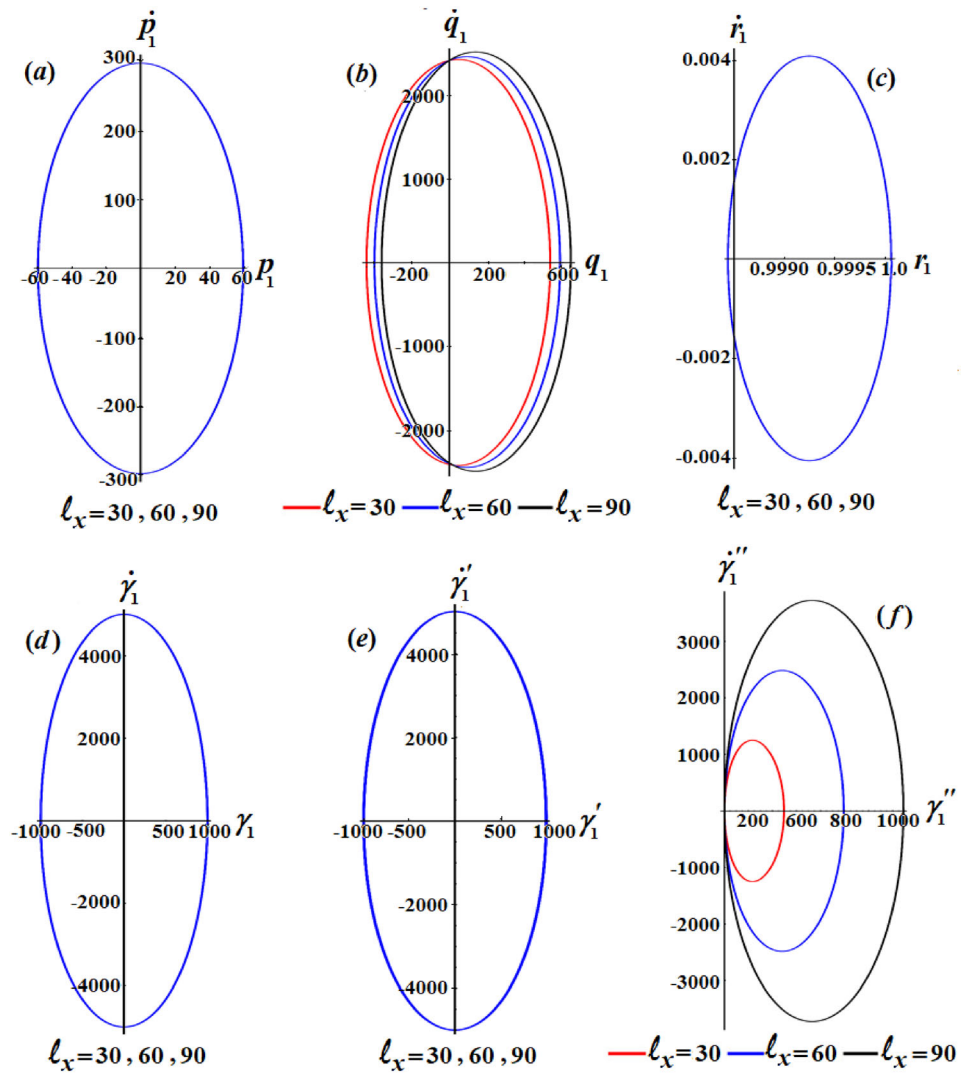
$$\begin{aligned} \theta_1(t) &= -y_1 \cos r_0 t, \\ \theta_2(t) &= (y_1 y_3 - a \lambda - x'_0) \cos r_0 t - (b X a^{-1} + 1) y'_0 \sin r_0 t \\ &\quad - \frac{1}{2} \tan \theta_0 (a \lambda_1 + b X \lambda_2 + \frac{1}{2} k C_1) \cos 2r_0 t, \\ \psi_1(t) &= 0, \\ \psi_2(t) &= r_0^{-1} (\Omega^{-2} x'_0 b^{-1} A_1 \sin r_0 t - A_1^{-1} a^{-1} y'_0 \cos r_0 t) \\ &\quad + \frac{1}{4} \tan \theta_0 [\lambda_1 (2t + r_0^{-1} \sin 2r_0 t) \\ &\quad + \lambda_2 (r_0^{-1} A_1^{-1} \sin 2r_0 t - 2X t)], \\ \psi_3(t) &= \frac{1}{4} X y_1 \tan \theta_0 \{ a^{-1} y'_0 (2 \cos r_0 t - r_0^{-1} \cos 2r_0 t) - k A_1 \tan \theta_0 [2t \\ &\quad - r_0^{-1} (\cos 2r_0 t - 4 \sin^3 r_0 t)] \}, \\ \phi_1(t) &= \psi_1(t), \quad \phi_2(t) = \psi_2(t), \quad \phi_4(t) = \psi_3(t), \\ \phi_3(t) &= x'_0 (r_0 t - \sin r_0 t) - y'_0 \cos r_0 t \\ &\quad + \frac{1}{8} k C_1 \tan \theta_0 (2r_0 t - \sin 2r_0 t). \end{aligned}$$

By carefully selecting the initial values  $\theta_0, \psi_0, \phi_0,$  and  $r_0,$  we can estimate the orientation of the RB’s motion in view of the previous Eqs. (43) of Euler’s angles. According to these equations, we can predict that the behavior of  $\theta$  and  $\varphi$  will be impacted and have periodic forms with the change of the GM, while the behavior of the angle  $\psi$  increases in the opposite direction.

### Numerical Simulations

The current section’s goal is to analyze the achieved solutions (41) and angles of Euler (43) at various values of the acted parameters on the RB’s motion. Consequently, the following relevant data in Table 1 are used to display the temporary motion and phase plane plots in various graphs.

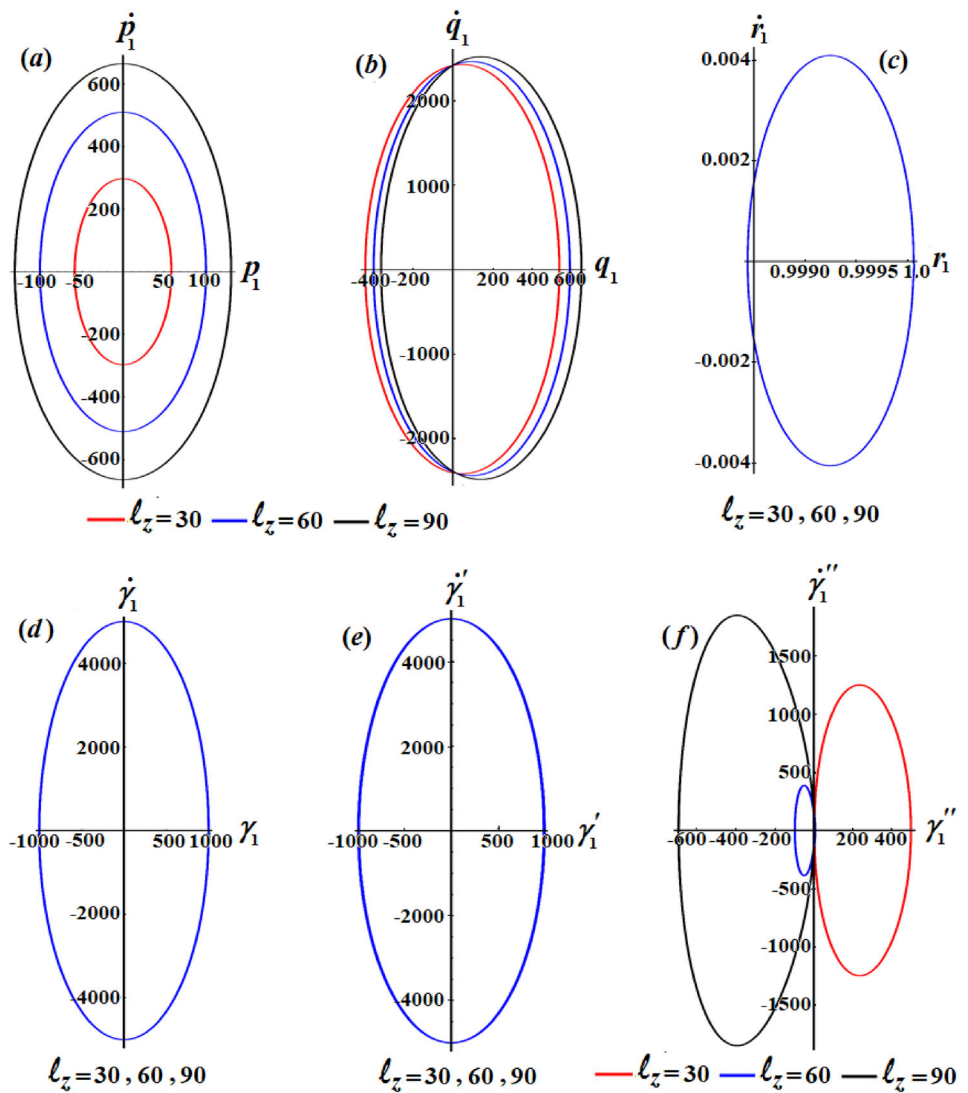
**Fig. 4** The phase plane diagrams of the solutions  $p_1, q_1, r_1, \gamma_1, \gamma_1'$ , and  $\gamma_1''$  at  $\ell_z = 30 \text{ kg m}^2 \text{ s}^{-1}$  with distinct values of  $\ell_x (= 30, 60, 90) \text{ kg m}^2 \text{ s}^{-1}$



The included curves in portions (a–f) of Figs. 2 and 3 depict the temporal histories of the solutions  $p_1, q_1, r_1, \gamma_1, \gamma_1'$ , and  $\gamma_1''$ . These curves are drawn when  $\ell_x = 30 \text{ kg m}^2 \text{ s}^{-1}$ ,  $\ell_z (= 30, 60, 90) \text{ kg m}^2 \text{ s}^{-1}$  and  $\ell_z = 30 \text{ kg m}^2 \text{ s}^{-1}$ ,  $\ell_x (= 30, 60, 90) \text{ kg m}^2 \text{ s}^{-1}$ , as presented in Figs. 2 and 3, respectively. It is notable that the represented waves of these solutions have the periodicity forms, as expected before, with the change of the projections of the GM on the main axes of inertia  $x$  and  $z$ . Moreover, the inspection of the portions of Fig. 2 shows that, the solutions  $q_1$  and  $\gamma_1'$  are influenced with the change of  $\ell_x$  values, where the amplitude's waves increase with the increase of  $\ell_x$  values, while the number of oscillations remains stationary. On the other hand, the other solutions are slightly affected to some extent with the variation of  $\ell_x$  even though the curves of these solutions are also periodic. Curves of Fig. 3 illustrate that the waves describing the behavior of

$p_1, q_1$ , and  $\gamma_1''$  have been impacted with the various values of  $\ell_z$ , in which the waves' amplitudes increase with the increase of  $\ell_z$ , as displayed in portions (a) and (b) of Fig. 3, while the amplitudes of the waves illustrating the solution  $\gamma_1''$  decrease with the increase of  $\ell_z$ , as drawn in Fig. 3f. The reminder waves of the solutions  $p_1, q_1$ , and  $\gamma_1'$  have no variation with the same values of  $\ell_z$ . These remarks agree with the obtained solutions (41). The phase plane plots of the explored curves in Figs. 2 and 3 are graphed in the corresponding portions of these figures with portions of Figs. 4 and 5. The latter Figs. 4 and 5 included closed curves which assert that the behaviors of the plotted solutions are stable and free of chaos. Based on the variation of the solutions with the values of  $\ell_x$  and  $\ell_z$ , we find that there is a corresponding change in plotted closed curves in Figs. 4 and 5.

**Fig. 5** The graphs of the solutions' phase plane when  $\ell_x = 30 \text{ kg m}^2 \text{ s}^{-1}$  according to the various values of  $\ell_z (= 30, 60, 90) \text{ kg m}^2 \text{ s}^{-1}$



The curves shown in portions of Figs. 6 and 7 are meant to demonstrate the temporal evolution of the angles  $\theta, \psi,$  and  $\phi$  under distinct values for  $\ell_x$  and  $\ell_z$ . The represented curves in portions (a–c) of Figs. 6 and 7 have been impacted with the change of the GM values. It is obvious that the waves of the angles  $\theta$  and  $\phi$  oscillate periodically, as seen in portions (a) and (b) of these figures, respectively. As contrasted to this, the behavior of the angle  $\psi$  has a negative direction when time goes on, as drawn in part (c) of the same figures. These curves are in full agreement with Eqs. (43).

### Conclusion

The positive impact of the NFF and the GM on the rotatory motion of a RB, about one of its fixed points has been examined for an analogs case of Lagrange’s gyroscope. The governing system of motion that consists of six non-linear DEs of first order has been derived using the principal equation of the angular momentum for the body’s motion. The three first integrals of this system related to energy, area, and geometric integral have been obtained. This system is reduced, using the APSP, to an appropriate one of two quasi-linear DEs of second order and one integral in terms of just two variables. It has been found



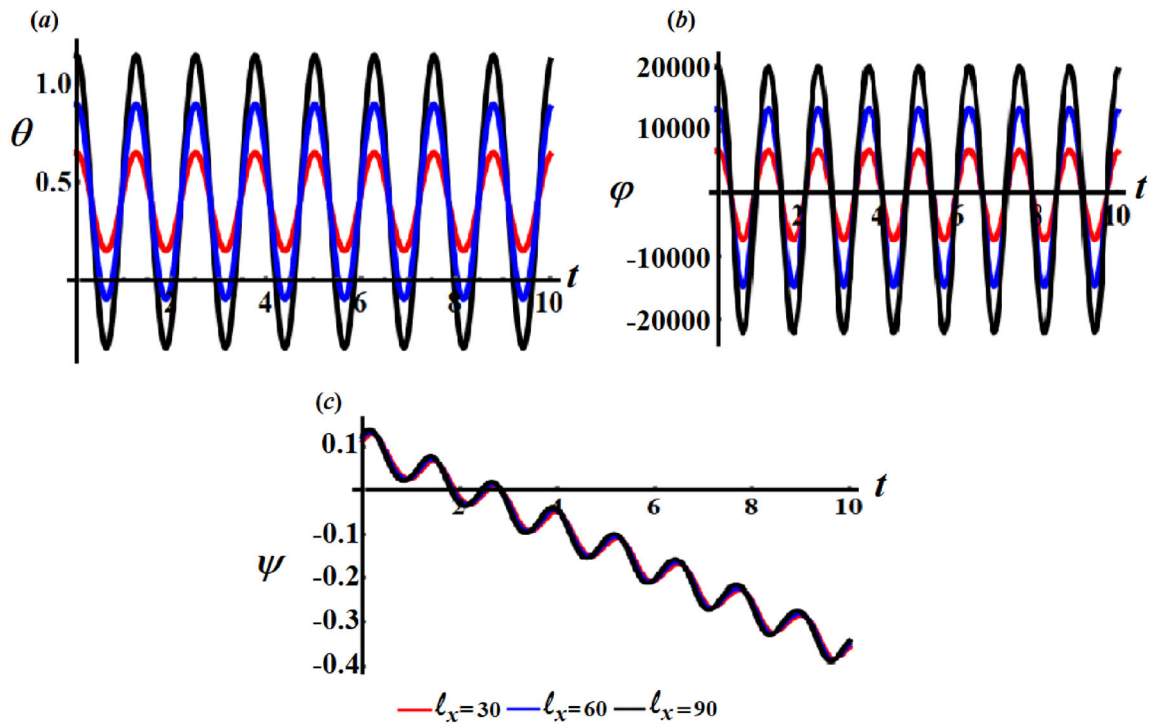


**Fig. 6** Reveals the variation of  $\theta(t)$ ,  $\phi(t)$ , and  $\psi(t)$  at  $\ell_z = 30 \text{ kg m}^2 \text{ s}^{-1}$  for various values of  $\ell_x (= 30, 60, 90) \text{ kg m}^2 \text{ s}^{-1}$

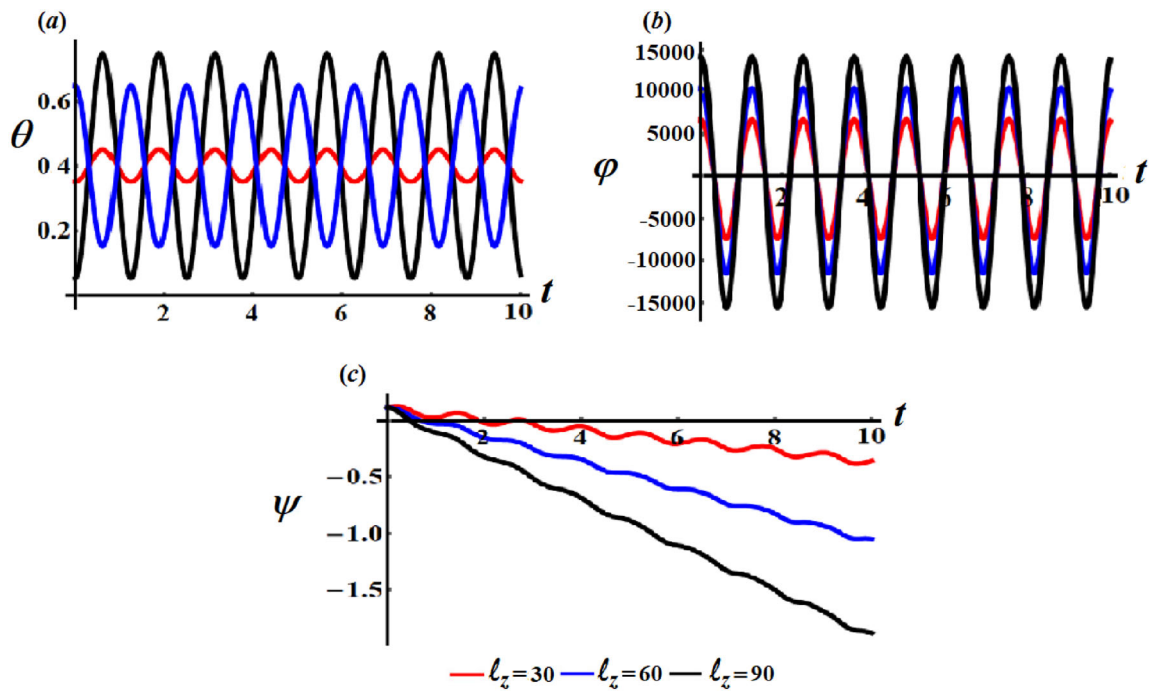


**Fig. 7** Shows the waves of  $\theta(t)$ ,  $\phi(t)$ , and  $\psi(t)$  at  $\ell_x = 30 \text{ kg m}^2 \text{ s}^{-1}$  for various values of  $\ell_z (= 30, 60, 90) \text{ kg m}^2 \text{ s}^{-1}$



that the obtained approximate solutions are valid for any value of the RB's frequency and do not have any singularities at all. The body's geometric interpretations have been estimated at any given time using Euler's angles. The achieved results have been drawn according to the values of the impacted parameters to show the behavior of the body's motion. Additionally, the stability of the dynamical motion is discussed using phase plane plots. These results are regarded as a generalization of those that were obtained in [7, 28, 30] for the absence of all applied forces and moments except NFF, and in [31] at ( $\ell_x = 0$ ,  $A \neq B$ ). This study presents an important contribution in a variety of critical domains, including the industrial uses of spacecraft, aircraft, and submarines.

**Acknowledgements** No official backing for this study came from any governmental body, business, or non-profit.

**Funding** Open access funding provided by The Science, Technology & Innovation Funding Authority (STDF) in cooperation with The Egyptian Knowledge Bank (EKB).

**Data Availability** In this study, no datasets were produced or examined; hence, data sharing is not appropriate.

## Declarations

**Conflict of Interest** No conflict of interest, according to the authors, has been disclosed.

**Open Access** This article is licensed under a Creative Commons Attribution 4.0 International License, which permits use, sharing, adaptation, distribution and reproduction in any medium or format, as long as you give appropriate credit to the original author(s) and the source, provide a link to the Creative Commons licence, and indicate if changes were made. The images or other third party material in this article are included in the article's Creative Commons licence, unless indicated otherwise in a credit line to the material. If material is not included in the article's Creative Commons licence and your intended use is not permitted by statutory regulation or exceeds the permitted use, you will need to obtain permission directly from the copyright holder. To view a copy of this licence, visit <http://creativecommons.org/licenses/by/4.0/>.

## References

1. Leimanis E (1965) The general problem of the motion of coupled rigid bodies about a fixed point. Springer, York
2. Yehia HM (2022) Rigid body dynamics: a Lagrangian approach. Birkhäuser, Springer Nature Switzerland AG
3. Malkin IG (1959) Some problems in the theory of nonlinear oscillations, United States Atomic Energy Commission. Technical Information Service, ABC-tr-3766
4. Bogoliubov NN, Mitropolsky YA (1961) Asymptotic methods in the theory of non-linear oscillations. Gordon and Breach
5. Nayfeh AH (1993) Introduction to perturbation techniques. Wiley-VCH
6. Nayfeh AH (2004) Perturbations methods. WILEY-VCH Verlag GmbH and Co. KGaA
7. Ismail AI (1996) On the application of Krylov-Bogoliubov-Mitropolski technique for treating the motion about a fixed point of a fast spinning heavy solid. ZFW 20(4):205–208
8. Amer TS, Ismail AI, Amer WS (2012) Application of the Krylov-Bogoliubov-Mitropolski technique for a rotating heavy solid under the influence of a gyrostatic moment. J Aerosp Eng 25(3):421–430
9. Amer TS, Abady IM (2017) On the application of KBM method for the 3-D motion of asymmetric rigid body. Nonlinear Dyn 89:1591–1609
10. Amer TS, Farag AM, Amer WS (2020) The dynamical motion of a rigid body for the case of ellipsoid inertia close to ellipsoid of rotation. Mech Res Commu 108:103583
11. Awrejcewicz J, Starosta R, Kamińska GS (2013) Asymptotic analysis of resonances in nonlinear vibrations of the 3-dof pendulum. Differ Equ Dyn Syst 21(1–2):123–140
12. El-Sabaa FM, Amer TS, Gad HM, Bek MA (2020) On the motion of a damped rigid body near resonances under the influence of harmonically external force and moments. Results Phys 19:103352
13. Amer TS, Bek MA, Abouhmr MK (2018) On the vibrational analysis for the motion of a harmonically damped rigid body pendulum. Nonlinear Dyn 91(4):2485–2502
14. Strogatz SH (2015) Nonlinear dynamics and chaos: with applications to physics, biology, chemistry, and engineering, 2nd edn. Princeton University Press
15. Amer TS (2017) The dynamical behavior of a rigid body relative equilibrium position. Adv Math Phys 2017:1–13
16. Awrejcewicz J, Kudra G (2005) Modeling, numerical analysis and application of triple physical pendulum with rigid limiters of motion. Arch Appl Mech 74:746–753
17. Awrejcewicz J, Supel B, Lamarque CH, Kudra G, Wasilewski G, Olejnik P (2008) Numerical and experimental study of regular and chaotic motion of triple physical pendulum. Int J Bifurc Chaos 18(10):2883–2915
18. Akulenko LD, Leshchenko DD, Chernousko FL (1986) Perturbed motions of a rigid body that are close to regular precession. Izv Akad Nauk SSSR MTT 21(5):3–10
19. Akulenko LD, Leshchenko DD, Kozachenko TA (2002) Evolution of rotations of a rigid body under the action of restoring and control moments. J Comput Syst Sci 41(5):868–874
20. Amer TS, Abady IM (2018) On the motion of a gyro in the presence of a Newtonian force field and applied moments. Math Mech Solids 23(9):1263–1273
21. Ismail AI, Amer TS, El Banna SA (2012) Electromagnetic gyroscopic motion. J Appl Math 2012:1–14
22. Amer TS (2008) On the rotational motion of a gyrost at about a fixed point with mass distribution. Nonlinear Dyn 54:189–198
23. Amer TS (2016) The rotational motion of the electromagnetic symmetric rigid body. Appl Math Inf Sci 10(4):1453–1464
24. Akulenko LD, Leshchenko DD, Chernousko FL (1979) Perturbed motions of a rigid body, close to the Lagrange case. J Appl Math Mech 43(5):829–837
25. Akulenko LD, Zinkevich YAS, Kozachenko TA, Leshchenko DD (2017) The evolution of the motions of a rigid body close to the Lagrange case under the action of an unsteady torque. J Appl Math Mech 81(2):79–84
26. Amer WS (2019) The dynamical motion of a gyroscope subjected to applied moments. Results Phys 12:1429–1435
27. Chernousko FL, Akulenko LD, Leshchenko DD (2017) Evolution of motions of a rigid body about its center of mass. Springer International Publishing AG
28. Iu A, Arkhangel'skii (1963) On the motion about a fixed point of a fast spinning heavy solid. J Appl Math Mech 27:1314–1333

29. Ismail AI (1998) The motion of a fast spinning disc which comes out from the limiting case. *Comput Methods Appl Mech Engrg* 16:67–76
30. El-Barki FA, Ismail AI (1995) Limiting case for the motion of a rigid body about a fixed point in the Newtonian force field. *ZAMM* 75(11):821–829
31. Ismail AI, Amer TS (2002) The fast spinning motion of a rigid body in the presence of a gyrostatic momentum. *Acta Mech* 154:31–46
32. Amer TS (2004) Motion of a rigid body analogous to the case of Euler and Poincaré. *Analysis* 24:305–315
33. Amer TS, Amer WS (2018) The rotational motion of a symmetric rigid body similar to Kovalevskaya's case. *Iran J Sci Technol Trans Sci* 42(3):1427–1438
34. He JH, Amer TS, El-Kafly HF, Galal AA (2022) Modelling of the rotational motion of 6-DOF rigid body according to the Bobylev-Steklov conditions. *Results Phys* 35:105391
35. Farag AM, Amer TS, Amer WS (2022) The periodic solutions of a symmetric charged gyrostic for a slightly relocated center of mass. *Alex Eng J* 61:7155–7170
36. Elfimov VS (1978) Existence of periodic solutions of equations of motion of a solid body similar to the Lagrange gyroscope. *J Appl Math Mech* 42(2):262–269
37. Amer TS (2008) On the motion of a gyrostic similar to Lagrange's gyroscope under the influence of a gyrostatic moment vector. *Nonlinear Dyn* 54:249–262
38. Amer WS (2017) On the motion of a flywheel in the presence of attracting center. *Results Phys* 7:1214–1220
39. Amer WS (2021) Modelling and analyzing the rotatory motion of a symmetric gyrostic subjected to a Newtonian and magnetic fields. *Results Phys* 24:104102
40. Yang XD, Liu M, Zhang W, Qian YJ, Melnik RV (2016) On the perturbation methods for vibration analysis of linear time-varying systems. *Int J Appl Mech* 8(3):1650035
41. Liu M, Li Z, Yang X, Zhang W, Lim CW (2020) Dynamic analysis of a deployable/retractable damped cantilever beam. *Appl Math Mech* 41(9):1321–1332
42. Ismail AI, Amer TS, Amer WS (2023) Advanced investigations of a restricted gyrostatic motion. *J Low Freq Noise Vib Active Control*. <https://doi.org/10.1177/14613484231160135>
43. Ismail AI, Amer TS, Amer WS (2023) Sufficiently small rotations of Lagrange's gyro. *J Low Freq Noise Vib Active Control*. <https://doi.org/10.1177/14613484231162447>
44. Galal AA (2022) Free rotation of a rigid mass carrying a rotor with an internal torque. *J Vib Eng Technol*. <https://doi.org/10.1007/s42417-022-00772-w>
45. Amer TS, El-Sabaa FM, Sallam AA, Abady IM (2023) Studying the vibrational motion of a rotating symmetrically charged solid body subjected to external forces and moments. *Math Comput Simul* 210:120–146
46. El-Sabaa FM, Amer TS, Sallam AA, Abady IM (2022) Modeling of the optimal deceleration for the rotatory motion of asymmetric rigid body. *Math Comput Simul* 198:407–425
47. El-Sabaa FM, Amer TS, Sallam AA, Abady IM (2022) Modeling a semi-optimal deceleration of a rigid body rotational motion in a resisting medium. *Sci Rep* 12:18916
48. Amer TS, Amer WS, El-Kafly H (2022) Studying the influence of external moment and force on a disc's motion. *Sci Rep* 12:16942

**Publisher's Note** Springer Nature remains neutral with regard to jurisdictional claims in published maps and institutional affiliations.